# Geranylgeranylated SNAREs Are Dominant Inhibitors of Membrane Fusion

**Eric Grote,* Misuzu Baba,‡ Yoshinori Ohsumi,§ and Peter J. Novick***

*Department of Cell Biology, Yale University School of Medicine, New Haven, Connecticut 06520; ‡Department of Chemical and Biological Sciences, Faculty of Science, Japan Women's University, Tokyo 112-8681, Japan; §Department of Cell Biology, National Institute for Basic Biology, Okazaki 444-8585, Japan

***Abstract.*** Exocytosis in yeast requires the assembly of the secretory vesicle soluble *N*-ethylmaleimide–sensitive factor attachment protein receptor (v-SNARE) Sncp and the plasma membrane t-SNAREs Ssop and Sec9p into a SNARE complex. High-level expression of mutant Snc1 or Sso2 proteins that have a COOH-terminal geranylgeranylation signal instead of a transmembrane domain inhibits exocytosis at a stage after vesicle docking. The mutant SNARE proteins are membrane associated, correctly targeted, assemble into SNARE complexes, and do not interfere with the incorporation of wild-type SNARE proteins into complexes. Mutant SNARE complexes recruit GFP-Sec1p to sites of exocytosis and can be disassembled by the Sec18p ATPase. Heterotrimeric SNARE complexes assembled from both wild-type and mutant SNAREs are present in heterogeneous higher-order complexes containing Sec1p that sediment at greater than 20S. Based on a structural analogy between geranylgeranylated SNAREs and the GPI-HA mutant influenza virus fusion protein, we propose that the mutant SNAREs are fusion proteins unable to catalyze fusion of the distal leaflets of the secretory vesicle and plasma membrane. In support of this model, the inverted cone–shaped lipid lysophosphatidylcholine rescues secretion from SNARE mutant cells.

Key words: secretion • exocytosis • yeast • fusion pore • hemifusion

## *Introduction*

Fusion of lipid bilayers is essential for a variety of fundamental biological processes including the entry of enveloped viruses into cells and intracellular membrane traffic. Since there is a substantial energy barrier preventing spontaneous membrane fusion under physiological conditions, biological membrane fusion is mediated by fusion proteins. Fusion proteins have been identified and extensively characterized for several enveloped viruses, but the identity of the fusion proteins for intracellular membrane fusion has not been conclusively established. Intracellular membrane fusion is a multistep process in which the two membranes must be correctly targeted and docked before fusion can occur. Many of the proteins implicated in the process of membrane fusion function at the targeting and docking stages. The most attractive candidate fusion proteins are the members of the soluble *N*-ethylmaleimide–sensitive factor (NSF)[1] attachment protein (SNAP) receptor (SNARE) family (Sollner et al., 1993b; Skehel and Wiley, 1998; Weber et al., 1998).

SNAREs were originally identified as membrane proteins that bound to the ATPase NSF via its cofactor α-SNAP (Sollner et al., 1993b). For fusion to occur, a trans-SNARE complex must assemble between v-SNAREs on a transport vesicle and t-SNAREs on its fusion target (Nichols et al., 1997). cis-SNARE complexes have also been observed where both transmembrane domains are present in the same membrane (Otto et al., 1997). These complexes may be remnants of previous membrane fusion events or may have simply assembled nonproductively. ATP hydrolysis by NSF leads to the disassembly of SNARE complexes and primes t-SNAREs for subsequent assembly into trans-SNARE complexes (Sollner et al., 1993a; Mayer et al., 1996; Ungermann et al., 1998a). The core of a SNARE complex is a four-stranded parallel α-helical bundle (Sutton et al., 1998). Transmembrane domains extending from the COOH terminus of the bundle are anchored in both the vesicle and target membranes (Hanson et al., 1997). The core of the SNARE complex also includes helices from proteins such as SNAP-25 that do not have a transmembrane domain but are associated with membranes often via a covalently attached lipid (Hess et al., 1992).

The fact that membranes must be closely apposed to be bridged by a trans-SNARE complex lends support to the

Address correspondence to Peter J. Novick, Dept. Cell Biology, Yale University School of Medicine, 333 Cedar St., New Haven, CT 06520-8002. Tel.: (203) 785-5871. Fax: (203) 785-7226. E-mail: peter.novick@yale.edu

[1]*Abbreviations used in this paper:* GFP, green fluorescent protein; gg-SNARE, geranylgeranylated SNARE; GPI, glycosylphosphatidylinositol; GST, glutathione *S*-transferase; HA, hemagglutinin; LPC, lysophosphatidylcholine; NSF, *N*-ethylmaleimide–sensitive factor; SNAP, soluble NSF attachment protein; SNARE, SNAP receptor.

notion that SNAREs function as fusion proteins. The data on this issue, however, are conflicting. SNARE-dependent fusion has been reconstituted with recombinantly expressed proteins incorporated into liposomes (Weber et al., 1998). However, it has also been reported that disassembly of trans-SNARE pairs by Sec18p, the yeast NSF, can occur before the completion of fusion in an in vitro assay of vacuole fusion (Ungermann et al., 1998b). To reconcile these observations, it has been suggested that the prefusion state of the SNARE complex has low affinity and is thus not detectable by standard assays (Chen et al., 1999).

For insight into how SNAREs might catalyze intracellular fusion, we have looked to the best understood form of membrane fusion, that mediated by the hemagglutinin (HA) protein of influenza virus (Bentz, 1993; White et al., 1996). Internalization of the virus to acidic endosomes triggers a conformational shift in HA2 resulting in insertion of the fusion peptide into the endosomal membrane. Fusion is thought to occur in two steps. First, the outer leaflets join to yield a hemifusion intermediate. Then, the inner leaflets join to form a fusion pore, which expands to allow entry of the viral core into the cytoplasm. The glycosylphosphatidylinositol (GPI)-HA mutant fusion protein is defective at the transition from the hemifusion intermediate to complete fusion (Kemble et al., 1993). In GPI-HA, the COOH-terminal transmembrane and cytoplasmic domains of HA have been replaced by a GPI membrane anchor. Unlike the COOH terminus of wild-type HA, the GPI anchor of GPI-HA is not inserted through the hydrophilic face of the cytoplasmic leaflet of the host cell. Thus, the GPI anchor can diffuse through the lipidic stalk connecting the hemifused membranes. Addition of chlorpromazine allows full fusion by GPI-HA (Melikyan et al., 1997; Chernomordik et al., 1999). Chlorpromazine is a membrane-permeant, inverted cone–shaped amphipath that preferentially accumulates in the cytoplasmic leaflet of the plasma membrane. In theory, adding chlorpromazine introduces positive curvature in the hemifusion diaphragm. This positive curvature then stabilizes small pores that form spontaneously, thereby increasing the probability that they will expand to complete fusion.

We have examined the role of SNARE transmembrane domains in membrane fusion by replacing the COOH-terminal transmembrane domains of the yeast exocytic SNAREs Snc2p and Sso2p (Sec9p has no transmembrane domain) with signals for addition of a geranylgeranyl lipid anchor. High expression of geranylgeranylated SNAREs (ggSNAREs) inhibits exocytosis at a stage after SNARE complex assembly. The secretory block in ggSNARE-expressing cells can be partially reversed by adding lysophosphatidylcholine (LPC), an inverted cone–shaped lipid that adds positive curvature to the outer leaflet of the plasma membrane. Thus, we conclude that SNAREs act at a late, lipid-sensitive step in membrane fusion and propose that ggSNAREs cannot catalyze merger of the distal leaflets of the secretory vesicle and plasma membrane.

## Materials and Methods

### Plasmids and Strain Construction

The *SNC-CIIL* integrating plasmid pNB974 was constructed by PCR amplification of *SNC1* using the reverse primer GCCGAAGCTTATCATAGAATTATACAACACATCTTCATTTTTAGATC to append sequences coding for CIIL-Stop (underlined) after Cys95. The PCR product was inserted between the BamHI and HindIII sites of pNB529, an integrating vector with a *GAL1* promoter, *ADH1* terminator, and *LEU2* selectable marker. The *SSO-CIIL* integrating plasmid pNB975 was constructed by PCR amplification of *SSO2* using the reverse primer CCAAGCTTATCATAGAATTATACAACATCTTATTTTGTTTTTTCTTGCTTTTCTGGC to append sequences coding for CIIL-Stop (underlined) after Cys270. Before inserting the *SSO-CIIL* PCR product into pNB529, the EcoRI site in the multicloning site of the vector was mutated by linearizing the plasmid with a partial EcoRI digest, and filling in the overhang using the Klenow subunit of DNA polymerase I. This mutagenesis allowed pNB975 to be linearized by digestion at the EcoRI site and integrated into the *LEU2* gene.

The *SEC+* host strain SP1α (*MATα his3 leu2 trp1 ade8 ura3*, NY1705) was constructed by transient transformation of a plasmid containing the HO endonuclease to change the mating type of the SP1 strain (Protopopov et al., 1993). The *SNC-CIIL* (NY1743) and *SSO-CIIL* (NY1704) strains were constructed by integration at the *LEU2* locus of SP1α. A yeast genomic library created by partial digestion of DBY939 genomic DNA with Sau3A and subcloning into yEP24 was used for the high-copy suppression screen. Other plasmid tested for suppression included the empty vector control (pRS426), pNB139 (*SEC4 CEN URA3*) and 2μ *URA3* plasmids with the *SEC1* (pNB680), *SEC9* (pNB592), *SEC17* (pSFN194), *SEC18* (pSFN199), *SSO2* (BVS), and *SNC2* (from the genomic library) genes.

Green fluorescent protein (GFP)-Sec1p fluorescence was observed in SP1α (NY1746), *SNC-CIIL* (NY1747), and *SSO-CIIL* (NY1748) strains transformed with pNB828 (Carr et al., 1999). The HA-tagged *SSO2* expressed in the *sec18-1 HA-SSO2* strain (*MATα sec18-1 HA-SSO2 ura3 leu2 his3*, NY1749) was constructed by the method of Schneider and colleagues (Schneider et al., 1995; Carr et al., 1999) in an L-a virus-free host strain. The *sec5 SSO-CIIL* strain (NY1272) was created by a genetic cross of NY504 (*MATα sec5-24 ura3 his4*) with SSO-CIIL transformed NY605 (*MATα leu2 ura3*). Strains were grown in media supplemented with 4% galactose, 4% raffinose, or 2% dextrose.

### Glycerol Gradients

40 $A_{600}$ units of yeast were lysed with glass beads in HKDNE buffer as described previously (Grote and Novick, 1999). 200 μl of cleared lysate (4 mg/ml) was layered over a linear 10–35% glycerol gradient in HKDNE and spun at 300,000 *g* (at $R_{max}$) for 5.3 h in an SW50.1 rotor (Beckman Coulter) at 4°C. 620-μl fractions were collected from the bottom of the gradient. The gradient fractions were diluted with an equal volume of HKDNE, and HA-Sso2p was collected by immunoprecipitation with the 12CA5 anti-HA monoclonal antibody. A parallel gradient was run with gel filtration markers (Bio-Rad Laboratories). Thyroglobulin (670 kD, 19S) sedimented to fraction 4.

### Secretion Assays

Secretion of $^{35}$S-labeled proteins was measured by a modification of the method of Gaynor and Emr (1997). 1.5 $A_{600}$ units of yeast cells from methionine-free medium were resuspended in 400 μl of methionine-free medium supplemented with 150 μCi [$^{35}$S]-ProMix™ cell labeling mix (Amersham Pharmacia Biotech) and labeled for 5 min at 30°C or 37°C as indicated. The labeling period was stopped by the addition of 44 μl 10× chase medium containing 7 mg/ml methionine, 4 mg/ml cysteine, 0.6 mg/ml BSA, and 10 mM PMSF. When indicated, freshly dissolved LPC (Avanti Polar Lipids, Inc.) was added to a final concentration of 0.3 mM. To collect secreted proteins, the cells were pelleted and 400 μl of supernatant was added to 40 μl of 100% TCA, 1 mg/ml deoxycholate, and precipitated for at least 30 min on ice. The precipitates were washed twice with acetone (−20°C), air dried, resuspended in Laemmli sample buffer, boiled for 5 min, and run on a 10% SDS-polyacrylamide gel. $^{35}$S-labeled proteins were quantified using a Storm™ system (Molecular Dynamics).

### Other Methods

Glutathione *S*-transferase (GST)-Snc-CIIL and GST-Sso-CIIL were purified from *Escherichia coli* and labeled with $^{3}$H-GGPP by the method of Jiang et al. (1993). Procedures for SNARE coimmunoprecipitation and immunoblotting have been described previously (Grote and Novick, 1999). GFP-Sec1p visualization followed the method of Carr et al. (1999) as modified (Grote et al., 2000, this issue). FM4-64 endocytosis was observed by the method of Vida and Emr (1995). CPY maturation was measured by the method of Govindan et al. (1995) except that the samples were not frozen and thawed before lysis. Immunofluorescent staining of Sec4p was by the method of Walch-Solimena et al. (1997) using a 63× ob-

jective. Samples were prepared for electron microscopy as described previously (Baba et al., 1997), and ultrathin sections were examined with a Hitachi H-800 electron microscope at 125 kV.

## Results

### Dominant-negative Lipid-anchored SNAREs

As a test of the role of SNARE transmembrane domains in the process of membrane fusion, we replaced the COOH-terminal transmembrane domain of the v-SNARE Snc2p with a CIIL signal coding for addition of a geranylgeranyl isoprenyl group (Moores et al., 1991). To demonstrate activity of the CIIL signal, we compared incorporation of [$^3$H]geranylgeranyl pyrophosphate into Snc-CIIL and the soluble cytoplasmic domain of Snc2p. Snc-CIIL was purified as an $NH_2$-terminal tagged GST fusion protein from *E. coli*. In the presence of lysate from wild-type yeast expressing type II geranylgeranyltransferase, [$^3$H]geranylgeranyl pyrophosphate was attached to the COOH terminus of Snc-CIIL, but not to the unmodified Snc2p cytoplasmic domain or to COOH-terminally truncated proteolytic fragments of Snc-CIIL (Fig. 1 a).

The *SNC-CIIL* gene was inserted behind a *GAL1* promoter in a yeast integrating vector and integrated at the *LEU2* locus of *SEC+* yeast. Expression of the native Snc1 and Snc2 proteins was not perturbed in the *SNC-CIIL* transformed strain (data not shown). To determine if replacing the transmembrane domain of Snc2p altered its intracellular targeting, we observed the intracellular distribution of Snc-CIIL by subcellular fractionation and immunofluorescent microscopy. In the first approach, wild-type control cells and cells expressing Snc-CIIL were lysed in detergent-free buffer, and the homogenates were fractionated by standard methods including differential centrifugation, velocity sedimentation in glycerol gradients, and sedimentation and floatation to equilibrium density on sucrose gradients. By all four fractionation methods Snc-CIIL, which migrates more rapidly than wild-type Sncp on polyacrylamide gels, was observed in the same fractions as the native Snc proteins. Furthermore, Snc-CIIL expression did not significantly alter the fractionation pattern of wild-type Sncp at an early time point after inducing expression by shifting to galactose medium (data not shown). Immunofluorescent staining of highly expressed Snc-CIIL with anti-Sncp antibodies was compared with the less intense staining pattern of Sncp in wild-type cells. In both cell types, labeling was observed on the cell surface and on punctate structures in the cytoplasm (data not shown). When *sncΔ* cells were stained with anti-Snc antibodies, only weak background fluorescence was observed. We conclude that geranylgeranylation of Sncp is sufficient for membrane attachment and does not disturb the normal targeting of Sncp to secretory vesicles and the plasma membrane. Snc-CIIL is probably transported to the plasma membrane via the conventional secretory pathway after posttranslational insertion into the ER like the prenylated protein N-Ras (Choy et al., 1999).

Induction of high-level Snc-CIIL expression with galactose significantly reduced the growth rate of *SNC-CIIL* cells compared with wild-type controls. However, if *SNC-CIIL* cells were grown for several generations in YP glucose medium before plating on YP galactose plates, spontaneous revertants were frequently observed. Snc-CIIL expression was measured in the parent strain and in 60 spontaneous revertants by Western blotting. In the parent strain, after 8 h induction with galactose the amount of Snc-CIIL expressed was at least five times greater than the combined expression level of the native Snc1 and Snc2 proteins. By contrast, Snc-CIIL expression was lost in 59 of 60 spontaneous revertants. The expression level of Snc-CIIL in the remaining revertant was reduced to a level equivalent to that of the native Snc proteins. Thus, Snc-CIIL is a dose-dependent inhibitor of growth.

In an attempt to identify Sncp interacting proteins, we screened a multicopy genomic library for genes that suppress *SNC-CIIL* when overexpressed. 10 suppressing plasmids were isolated. Five of these plasmids contained either the *SNC1* or *SNC2* genes. The remaining plasmids interfered with Snc-CIIL expression. We conclude that the crit-

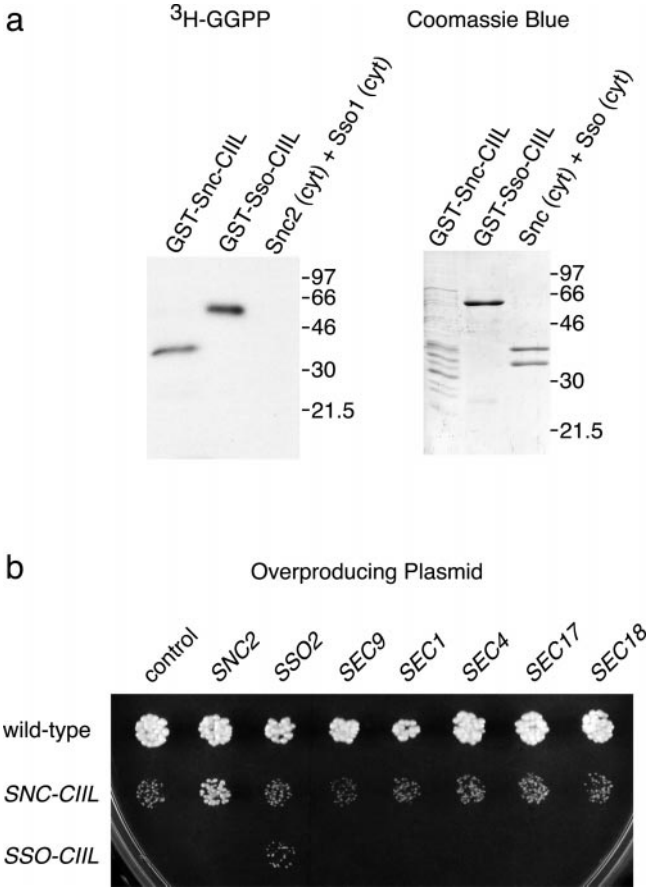


*Figure 1.* (a) Geranylgeranylation of Snc-CIIL and Sso-CIIL. GST-Snc-CIIL, GST-Sso-CIIL, and a 1:1 mixture of the Snc2p and Sso1p cytoplasmic domains were incubated with wild-type yeast lysate and [$^3$H]geranylgeranyl pyrophosphate for 30 min at 30°C. The reactions were run on a polyacrylamide gel, and geranylgeranylated products were detected by autoradiography. Only 10% of the GST-Sso-CIIL sample was loaded on the gel exposed for autoradiography. The input proteins were run on a second gel and stained with Coomassie blue. Only the full-length GST–Snc-CIIL protein at 38 kD contains the COOH-terminal CIIL signal; degradation products were not labelled with $^3$H-GGPP. (b) Growth phenotype and suppression of strains expressing Snc-CIIL and Sso-CIIL. *SNC-CIIL* and *SSO-CIIL* under regulatory control of a *GAL1* promoter were integrated at the *LEU2* locus of *SEC+* yeast (SP1). The control, *SNC-CIIL*, and *SSO-CIIL* strains were then transformed with *URA3* episomal plasmids directing overexpression of potential interacting proteins. The transformants were stamped onto synthetic complete (SC) galactose − uracil plates and grown for 5 d at 30°C.

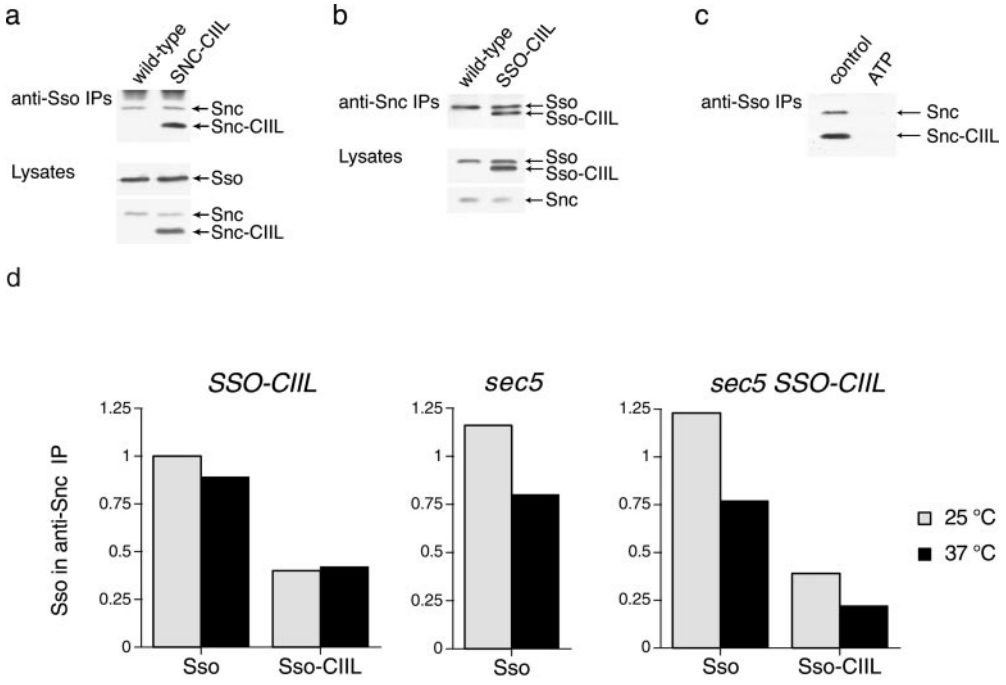


*Figure 2.* Assembly of ggSNAREs into SNARE complexes. (a) Coimmunoprecipitation of Snc-CIIL and Sncp with Ssop. Ssop was immunoprecipitated from cleared detergent lysates of wild-type and *SNC-CIIL* cells grown in YP galactose for 4 h at 30°C. Sncp and Snc-CIIL coprecipitating with Ssop and in 1% of the volume of lysate used for each immunoprecipitate were detected by immunoblotting. (b) Coimmunoprecipitation of Sso-CIIL and Ssop with Snc. Sncp was immunoprecipitated from cleared detergent lysates of wild-type and *SSO-CIIL* cells. Ssop and Sso-CIIL coprecipitating with Sncp and in 1% of the volume of lysate used for each immunoprecipitate were detected by immunoblotting. (c) Addition of ATP to lysates prevents coprecipitation of Snc-CIIL and Sncp with Ssop. Two lysates were prepared from *SNC-CIIL* cells grown for 4 h in YP galactose. For the control lysate, cells were collected in ice-cold Tris (pH 7.5) buffer containing 20 mM $NaN_3$ and 20 mM NaF to deplete intracellular pools of ATP and lysed in buffer containing 1 mM EDTA as in a and b above. For the +ATP lysate, cells were collected in buffer without $NaN_3$ or NaF and lysed in buffer with 2.5 mM ATP, 2 mM $MgCl_2$, and an ATP regenerating system. Sncp and Snc-CIIL coimmunoprecipitating with Sso were detected by immunoblotting as above. (d) SNARE complex levels in wild-type and *sec5-24* mutant cells. *SSO-CIIL*, *sec5-24*, and *sec5-24 SSO-CIIL* double mutant cells were grown in YP galactose plus raffinose for 3 h at 25°C to induce low level expression of Sso-CIIL and then shifted to 37°C for 30 min. Ssop and Sso-CIIL coprecipitating with Sncp were detected by immunoblotting and quantified by densitometry. The expression levels of Sncp and Ssop were equal in each strain, and the expression level of Sso-CIIL was equal in the wild-type and *sec5-24* mutant strains.

ical parameter for Snc-CIIL toxicity is the ratio of Snc-CIIL to wild-type Sncp expressed.

To compare the role of v-SNARE and t-SNARE transmembrane domains, we replaced the COOH-terminal transmembrane domain of the t-SNARE Sso2p with a geranylgeranylation signal. GST-Sso-CIIL, but not the cytoplasmic domain of Sso2p, could be labeled in vitro with [$^3$H]geranylgeranyl pyrophosphate in the presence of geranylgeranyltransferase from a yeast lysate (Fig. 1 a). High-level Sso-CIIL expression is an even stronger inhibitor of growth than high level Snc-CIIL expression. In contrast, a high level expression of the soluble cytoplasmic domain of Sso2p did not inhibit growth, emphasizing the importance of membrane attachment by the lipid anchor. To compare the mechanism of growth inhibition by Snc-CIIL and Sso-CIIL, we directly tested for suppression of the two mutants by overexpressing proteins likely to interact with Sncp and Ssop (Fig. 1 b). We found that *SNC2* suppresses *SNC-CIIL* but not *SSO-CIIL*, whereas *SSO2* suppresses *SSO-CIIL* but not *SNC-CIIL*. Thus, for Sso-CIIL as well as Snc-CIIL, a high ratio of geranylgeranylated to wild-type SNARE protein is implicated in the growth inhibition. Plasmids directing overexpression of other known SNARE complex interacting proteins, including Sec9p, Sec1p, Sec17p, or Sec18p, did not suppress either *SNC-CIIL* or *SSO-CIIL*. In addition, Sec4p overproduction, which suppresses most of the post-Golgi–blocked temperature-sensitive *sec* alleles (Salminen and Novick, 1987), did not suppress *SNC-CIIL* or *SSO-CIIL*. Thus, the ggSNAREs are not inhibiting growth by titering out other components known to interact with exocytic SNARE proteins.

One caveat concerning the interpretation of these results is that overexpression of wild-type t-SNAREs inhibits membrane transport in several other systems (Dascher et al., 1994; Bittner et al., 1996; Wu et al., 1998). Consistent with these reports, we found that massive overproduction of Sso2p from a *GAL1* promoter partially inhibited growth (data not shown). However, since moderate overproduction of Sso2p from a multicopy plasmid suppressed the growth defect of an *SSO-CIIL* strain, wild-type Sso2p and Sso-CIIL must inhibit growth by distinct mechanisms.

### *SNARE Complex Assembly with ggSNAREs*

We next tested whether the ggSNAREs assemble into SNARE complexes. Replacing the transmembrane domains of Sncp and Ssop with lipid anchors does not alter the domains essential for SNARE complex assembly in vitro, but assembly in yeast is subject to additional levels of regulation. We have previously documented that ~1% of the total Ssop in *SEC+* cells coimmunoprecipitates with Sncp and a similar fraction of the total Sncp coprecipitates with Ssop (Grote and Novick, 1999). Coimmunoprecipitation is a valid measure of SNARE complex assembly during exocytosis because the amount of Ssop coprecipitated with Sncp is reduced in mutant yeast strains with defects that prevent secretory vesicle docking with the plasma membrane (Grote and Novick, 1999; Grote et al., 2000,

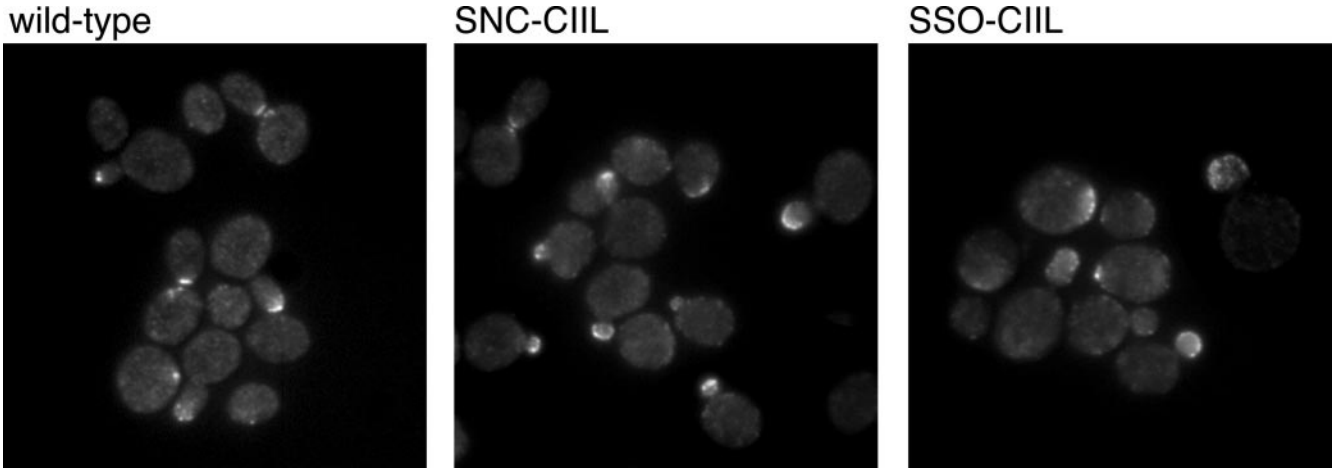


*Figure 3.* GFP-Sec1p fluorescence. GFP was integrated at the 5′ end of the *SEC1* gene in wild-type, *SNC-CIIL*, and *SSO-CIIL* cells. Transformants were grown to early log phase in YP raffinose and then transferred to YP galactose medium for 4 h at 30°C. The cells were fixed with methanol to enhance the GFP signal.

this issue). Immunoprecipitation of Ssop from cells expressing Snc-CIIL resulted in coimmunoprecipitation of both Snc-CIIL and wild-type Sncp (Fig. 2 a). Similarly, immunoprecipitation of Sncp from cells expressing Sso-CIIL resulted in coimmunoprecipitation of both Sso-CIIL and wild-type Ssop (Fig. 2 b). One way that ggSNAREs might inhibit secretion is by competing with wild-type SNARE proteins for assembly into SNARE complexes. Interestingly, Snc-CIIL expression did not affect the amount of native Sncp associated with Ssop, and Sso-CIIL expression did not affect the amount of native Ssop associated with Sncp. Thus, cells expressing ggSNAREs contain wild-type as well as mutant SNARE complexes.

The NSF ATPase disassembles SNARE complexes (Sollner et al., 1993a). In yeast, we and others have observed that addition of ATP and an ATP regenerating system to lysates induces disassembly of SNARE complexes by the NSF homologue Sec18p (Ungermann et al., 1998a; Carr et al., 1999). To test whether geranylgeranylation of SNAREs inhibits SNARE complex disassembly, we prepared lysates with and without ATP from *SNC-CIIL* cells. Neither Sncp nor Snc-CIIL coprecipitated with Ssop in lysates prepared under SNARE disassembly (+ATP) conditions (Fig. 2 c). Therefore, the geranylgeranyl membrane anchor does not interfere with SNARE complex disassembly in lysates.

Exocytic SNARE complex assembly depends on continued traffic through the secretory pathway (Grote and Novick, 1999). Thus, SNARE complexes fail to assemble at 37°C in the *sec5-24* temperature-sensitive mutant (Grote et al., 2000). Since Sec5p is a component of the exocyst complex that tethers secretory vesicles to the plasma membrane (TerBush et al., 1996; Guo et al., 1999), we concluded that vesicle tethering is required for exocytic SNARE complex assembly. To determine if vesicle tethering is also required for the assembly of SNARE complexes containing Sso-CIIL, we observed SNARE complexes in a *sec5-24 SSO-CIIL* strain. To avoid complications arising from the dominant-negative effects of high-level Sso-CIIL expression, the experiment was performed at an early time point after galactose addition before Sso-CIIL had a measurable effect on the growth rate. In addition, raffinose was included in the induction medium to reduce Sso-CIIL expression and minimize the disruptive effect of changing carbon sources. A 30% reduction in the binding of Ssop to Sncp was observed in *sec5-24* cells after shifting to 37°C in YP galactose plus raffinose. This effect is small compared with the 90% reduction in SNARE complex levels observed in the same cells grown in YP glucose (Grote et al., 2000). In the absence of glucose, a reduced growth rate and partial translocation of Ssop from the plasma membrane to intracellular vesicles (data not shown) may contribute to the reduced response of SNARE complexes to the temperature shift. Nevertheless, when *sec5-24 SSO-CIIL* cells were shifted to 37°C, there was a reduction in binding of both Sso-CIIL and Ssop to Sncp, and this reduction was equivalent to the reduction in binding of Ssop to Sncp in *sec5-24* cells not expressing Sso-CIIL. Furthermore, binding of Sso-CIIL to Sncp was not reduced at 37°C in a *SEC5 SSO-CIIL* strain (Fig. 2 d). Because the *sec5-24* mutation has equivalent effects on SNARE complexes containing Sso-CIIL and wild-type Ssop, we conclude that tethering of secretory vesicles to the plasma membrane precedes the assembly of SNARE complexes between Sncp and Sso-CIILp at the plasma membrane.

Sec1p binds to assembled Sncp/Ssop/Sec9p SNARE complexes and is targeted to sites of exocytosis in the tips of emerging buds and at mother–daughter necks in dividing cells (Carr et al., 1999). The fluorescence pattern of GFP-Sec1p was observed in *SNC-CIIL* and *SSO-CIIL* cells to determine the effect of ggSNARE expression on Sec1p targeting. Expression of Snc-CIIL or Sso-CIIL did not interfere with the targeting of GFP-Sec1p to bud tips and necks. However, the region of bright GFP-Sec1p fluorescence extended over a larger area of the plasma membrane within the bud in ggSNARE-expressing cells (Fig. 3). Since the peak intensity was similar in wild-type and mutant cells, the total amount of GFP-Sec1p targeted to the plasma membrane in the bud appears to be greater in the mutant cells. Coimmunoprecipitation of Sec1p with SNARE complexes was also enhanced by ggSNARE expression (see below, and data not shown). Thus, Sec1p interacts with SNARE complexes containing ggSNAREs.

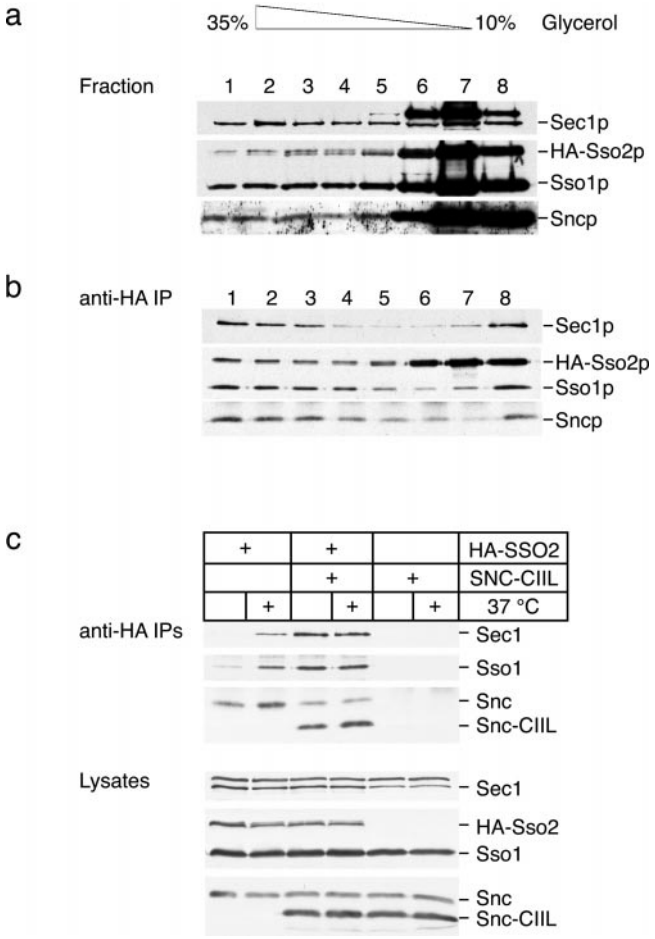


*Figure 4.* Multimeric SNARE complexes. (a) Sedimentation of detergent-solubilized yeast proteins on a glycerol velocity gradient. HA-SSO2 *sec18-1* cells were grown to log phase at 25°C and then shifted to 37°C for 10 min before lysis in buffer containing 0.5% NP-40. 200 μl of a cleared lysate was loaded on the top of a 5–35% glycerol gradient prepared in 0.5% NP-40 lysis buffer. After centrifugation at 300,000 *g* for 5.3 h, fractions were collected from the bottom of the gradient. An aliquot of each gradient fraction was run on an SDS-PAGE gel and probed for Sec1p, Ssop, and Sncp by immunoblotting. The upper band detected with the Sec1p antibody is not Sec1p. In an identical gradient run in parallel, thyroglobulin (19.6S) sedimented to a sharp peak in fraction 4. (b) Coprecipitation of Sec1p, Sec9p, Sso1p, and Sncp with HA-Sso2p from the glycerol gradient fractions. HA-Sso2p was immunoprecipitated from each gradient fraction in a using an anti-HA monoclonal antibody. (c) Coimmunoprecipitation of Sec1p, Sso1, and Sncp with HA-SSO2 is enhanced by Snc-CIIL expression. *HA-SSO2 sec18-1*, *SNC-CIIL HA-SSO2 sec18-1*, and *SNC-CIIL sec18-1* cells were grown for 4 h in YP galactose at 25°C. The cultures were split in two, and one aliquot was shifted to 37°C for 10 min before lysis. Anti-HA immunoprecipitates and 1% of the lysate were probed for Sec1p, HA-Sso2p, Sso1p, Sncp, and Snc-CIIL by immunoblotting. The HA-Sso2p band from the anti-HA immunoprecipitates was dissected away from the Sso1p band before probing with the anti-Sso antibody.

### *Higher-Order SNARE Complex Assembly*

SNARE proteins isolated from rat brains are found in 7S heterotrimeric VAMP/syntaxin/SNAP-25 complexes. 20S SNARE complexes are formed upon the addition of recombinantly expressed α-SNAP and NSF (Sollner et al., 1993a). To examine the sedimentation rate of yeast exocytic SNAREs, a detergent-solubilized yeast lysate was sedimented into a glycerol gradient. Centrifugation conditions were calibrated so that a 19.6S marker protein (thyroglobulin) sedimented to a peak near the center of the gradient in fraction 4, and purified recombinant monomeric Ssop cytoplasmic domain (Rice et al., 1997) was recovered from the top three fractions. The lysate was prepared from *sec18-1* cells shifted to 37°C before lysis to maximize the percentage of SNAREs incorporated into SNARE complexes. The majority of the Sncp, Sso1p, and HA-Sso2p sedimented at the rate expected for monomers, dimers, and small complexes, but a small percentage of the SNARE proteins sedimented more rapidly and were broadly distributed in the lower fractions of the gradient (Fig. 4 a).

The percentage of Ssop that sedimented at ≥20S in the glycerol gradient was similar to the percentage of Ssop bound to Sncp. Both rapid sedimentation and coprecipitation are enhanced in a *sec18-1* strain upon shift to 37°C and reduced in *sec4-8* strains (data not shown). To determine where SNARE complexes sediment in the glycerol gradient, HA-Sso2 was immunoprecipitated from an aliquot of each gradient fraction with an anti-HA antibody. The HA-Sso2–bound Sncp was enriched in the more rapidly sedimenting fractions, whereas the unbound Sncp sedimented as monomer (Fig. 4 b). HA-Sso2p–bound Sec1p and Sso1p were also enriched in the more rapidly sedimenting fractions. Coprecipitation of untagged Sso1p with HA-Sso2p is especially informative because it suggests that the rapidly sedimenting SNARE proteins are components of higher-order SNARE multimers containing at least two SNARE heterotrimers. However, since these SNARE complexes sediment heterogeneously and have not been purified, it is impossible to determine the precise stoichiometry of each component or to exclude the possibility that other unidentified proteins may associate with this pool of SNAREs.

A small fraction of the Sncp, Sec1p, and untagged Ssop in the top fraction of the glycerol gradient coprecipitated with HA-Sso2p (Fig. 4 b). These proteins were not present in a control anti-HA precipitation from the top fraction of a gradient prepared from an untagged *sec18-1* strain (data not shown). Since myoglobin, a 17-kD globular protein used as a standard, sedimented to a peak in the second fraction of an identical gradient (data not shown), the complexes in the top fraction of the gradient must be associated with a buoyant component such as a detergent-insoluble lipid raft.

If the assembly of SNARE trimers into higher-order multimers requires hydrophobic interactions mediated by transmembrane domains (Laage et al., 2000), ggSNAREs might be excluded from the multimeric SNARE complexes or might limit their assembly. Therefore, assembly of higher-order SNARE multimers was examined in cells expressing ggSNAREs. To streamline the assay for higher-order SNARE complex assembly, we tested for coimmunoprecipitation of Sso1p with HA-Sso2p (Fig. 4 c). As shown above, this interaction occurs primarily within the rapidly sedimenting complexes. To further validate the assay, we compared HA-Sso2p immunoprecipitates from *sec18-1* cells that were either maintained at the permissive

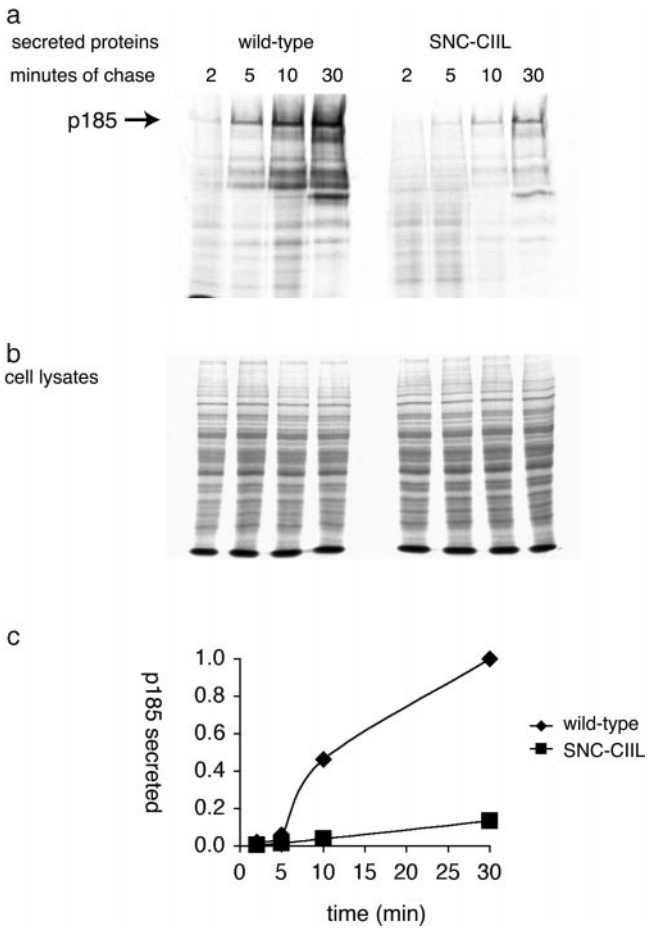


*Figure 5.* SNC-CIIL inhibits secretion. Snc-CIIL expression was induced for 6 h in SC galactose medium without methionine at 25°C. Cells were labeled for 5 min with [$^{35}$S]-ProMix, and chased with excess methionine and cysteine. Aliquots were removed at the indicated time points and separated into cell pellet and media fractions by centrifugation. (a) Media proteins collected by TCA precipitation and (b) cellular proteins released by glass bead lysis were run on SDS-PAGE gels. Autoradiographs were exposed to film for 4 d (secreted proteins) and 2 h (2% of lysate). (c) Secretion of the 185-kD protein (arrow in a) was quantified using a Storm™ PhosphorImaging system.

temperature of 25°C or shifted to 37°C for 10 min. As expected, the amount of Sso1p, Sncp, and Sec1p bound to HA-Sso2 increased when the mutant Sec18-1 protein was inactivated. When HA-Sso2p was immunoprecipitated from *SNC-CIIL* cells, both Sncp and Snc-CIIL coprecipitated, as shown in Fig. 2. The amount of Sso1p bound to HA-Sso2p also increased in Snc-CIIL–expressing cells. Therefore, cells expressing Snc-CIIL have more higher-order SNARE multimers in addition to more SNARE trimers. Consistent with the GFP-Sec1p fluorescence results (Fig. 3), the amount of Sec1p bound to HA-Sso2 also increased in the Snc-CIIL–expressing cells. Unexpectedly, blocking SNARE complex disassembly by shifting *sec18-1 SNC-CIIL* cells to 37°C before lysis resulted in only a small increase in the amount of Sec1p, Sso1p, and Sncp bound to HA-Sso2p. Since SNARE complex assembly depends on flux through the secretory pathway (Grote and Novick, 1999), one interpretation of this result is that an exocytosis block resulting from Snc-CIIL expression prevents additional SNARE complex assembly.

We also examined sedimentation of SNARE complexes from *SNC-CIIL* and *SSO-CIIL* cells into glycerol gradients. ggSNARE expression did not affect the sedimentation behavior of the wild-type SNAREs, and the behavior of the ggSNAREs and wild-type SNAREs was identical. In particular, <2% of the Snc-CIIL and Sso-CIIL sedimented at ≥20S, but the pools of both Snc-CIIL and Sso-CIIL in SNARE complexes were highly enriched in the rapidly sedimenting fractions (data not shown). We conclude that assembly of Sncp and Ssop into multimeric SNARE complexes is unaffected by replacement of the transmembrane domain with a lipid anchor.

### *ggSNAREs Inhibit Secretory Vesicle Fusion*

Since Sncp and Ssop are implicated in the final stage of secretion, we tested the effect of high level Snc-CIIL and Sso-CIIL expression on secretion. 6 h after Snc-CIIL induction, cells were metabolically labeled with a 5-min pulse of [$^{35}$S]methionine/cysteine and then chased for various periods of time. Proteins secreted into the media were concentrated by TCA precipitation and then separated on a polyacrylamide gel. The pattern of bands secreted by wild-type and *SNC-CIIL* cells was similar, but the rate of secretion was significantly slower in the *SNC-CIIL* cells (Fig. 5). No reduction in protein synthesis was observed. Similar results were observed for *SSO-CIIL* as shown below. Thus, the growth inhibitory effects of the ggSNAREs are coincident with an inhibition of secretion.

Because Sncp binds to several syntaxin-like t-SNAREs in addition to Ssop (Abeliovich et al., 1998; Holthuis et al., 1998; Grote and Novick, 1999), we tested whether transport to the vacuole is also inhibited by Snc-CIIL expression. Newly synthesized carboxypeptidase Y was targeted to vacuoles and processed to its mature form at the same rate in wild-type and *SNC-CIIL* cells after 4 h growth in galactose medium (data not shown). Similarly, transport of the fluorescent dye FM4-64 from the plasma membrane to vacuoles was normal in *SNC-CIIL* cells after 4 h growth in galactose (data not shown). Because secretion is inhibited at this time point by 50% in *SNC-CIIL* cells, we conclude that exocytosis is the first transport step to be inhibited by Snc-CIIL expression. However, after 10 h growth in galactose medium, FM4-64 was internalized, but was not transported to a single large vacuole (data not shown). This endocytic defect may be either a direct consequence of Snc-CIIL binding to endocytic t-SNAREs (Grote and Novick, 1999) or an indirect effect of the block in secretion.

To determine which stage of the secretory pathway is inhibited by ggSNARE expression, we began with testing for vesicle targeting by immunofluorescent staining of the vesicle-associated Rab GTPase Sec4p. Vesicle targeting defects in mutants that affect the actin cytoskeleton or prevent nucleotide exchange on Sec4p result in a loss of polarized Sec4p immunofluorescent staining (Walch-Solimena et al., 1997). In *SNC-CIIL* and *SSO-CIIL* cells, Sec4p fluorescence is concentrated in bud tips and mother–daughter necks as it is in *SEC+* yeast (Fig. 6). However, Sec4p staining is more intense and fills a larger area of the cytosol in the mutant cells. Thus, ggSNAREs

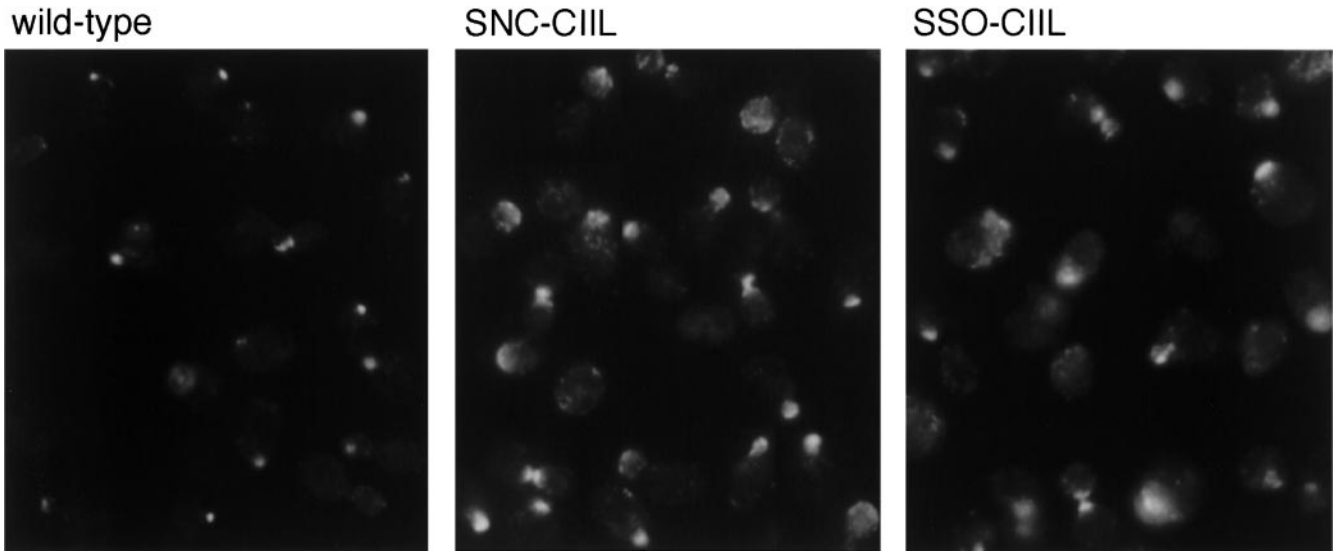


*Figure 6.* Immunofluorescent labeling of Sec4p in cells expressing Snc-CIIL and Sso-CIIL. Wild-type, *SNC-CIIL*, and *SSO-CIIL* cells were grown in YP galactose for 4 h at 30°C before fixation. Fixed cells were permeabilized with 0.1% SDS and then stained for Sec4p by indirect immunofluorescence. Some of the bud tips are above or below the plane of focus.

do not inhibit vesicle targeting but may cause an accumulation of vesicles that occupy a large fraction of the bud.

To test for secretory vesicle accumulation more directly, $OsO_4$/UAc-stained ultrathin sections were observed by transmission electron microscopy. There was a significant accumulation of 100-nm secretory vesicles in cells expressing Snc-CIIL or Sso-CIIL. We observed the time course of vesicle accumulation after induction of Sso-CIIL expression. 1 h after shifting to galactose medium, the small number (5–30) of vesicles observed were often located adjacent to the plasma membrane in the bud. After 2 h induction, hundreds of vesicles filled the entire bud and spilled over into the mother cell. At later time points, other abnormal membrane structures including enlarged secretory vesicles and Berkeley Bodies, swollen derivatives of the yeast Golgi, were observed (data not shown).

To look at higher resolution for evidence of vesicle docking, freeze-substituted samples were prepared for electron microscopy (Fig. 7). On these specimens, vesicles were often surrounded by a regularly spaced coat structure that excluded densely staining ribosomes. A small number of vesicles (five or less per cell cross-section) were located within 15 nm of the plasma membrane. These vesicles often bulged out towards the plasma membrane, suggesting a strong physical attachment. It is difficult to trace membranes at sites of contact between vesicles and the plasma membrane because ultrathin sections are 60-nm thick, whereas only 10 nm separates the two hydrophilic layers of phospholipid bilayer membranes. In some instances, distinct secretory and plasma membrane bilayers can be observed, but these may have been sectioned above or below the point of contact. In other images, the outer leaflet of the secretory vesicle and the inner leaflet of the plasma membrane appear to merge at the intersection point and in rare cases vanish. These images may represent the initiation of membrane fusion. No contacts were found where the outer leaflet of the plasma membrane and the inner leaflet of the vesicles coalesced to form a single extended bilayer. Thus, if exocytosis is arrested at a hemifusion intermediate in cells expressing ggSNAREs, the intermediate must either be short-lived or have a diameter less than the thickness of the sections. In addition, a similar number of vesicles closely apposed to the plasma membrane were observed in cells expressing the dominant-negative mutant *sec4-N34* (data not shown). GTP-Sec4p is known to be required for vesicle transport to bud tips (Walch-Solimena et al., 1997) and to bind to Sec15p, a component of the exocyst tethering complex (Guo et al., 1999). Furthermore, Sec4-N34 expression inhibits SNARE complex assembly (Grote and Novick, 1999). It is therefore possible that some of the vesicles that appear to be docked in ggSNARE cells have randomly localized adjacent to the plasma membrane.

### *LPC Rescues Secretion in SNC-CIIL and SSO-CIIL Cells*

The major difference between the lipid anchors of ggSNAREs and the transmembrane domains of wild-type SNAREs is that a geranylgeranyl group cannot interact with the hydrophilic portion of the distal leaflet of a phospholipid bilayer, whereas the transmembrane domain must interact with the distal leaflet because it spans the entire membrane and is followed by a short hydrophilic sequence. We reasoned that an agent that increases the fusion potential of the distal leaflet might rescue secretion from cells expressing ggSNAREs. 10:0 LPC is an inverted cone–shaped lipid with a bulky, positively charged choline head group and a single, 10-carbon saturated aliphatic chain. The choline head group prevents spontaneous transport of LPC across lipid bilayers, and there is no enzymatic LPC flip-flop across the yeast plasma membrane (Tang et al., 1996). Thus, LPC has the potential to induce positive curvature in the outer leaflet of the plasma membrane (Sheetz and Singer, 1974).

To assay for LPC-mediated suppression of the exocytic block, we pulse labeled cells with [$^{35}$S]methionine/cysteine and measured secretion of the labeled 185-kD protein identified in Fig. 5 in the presence or absence of LPC. An

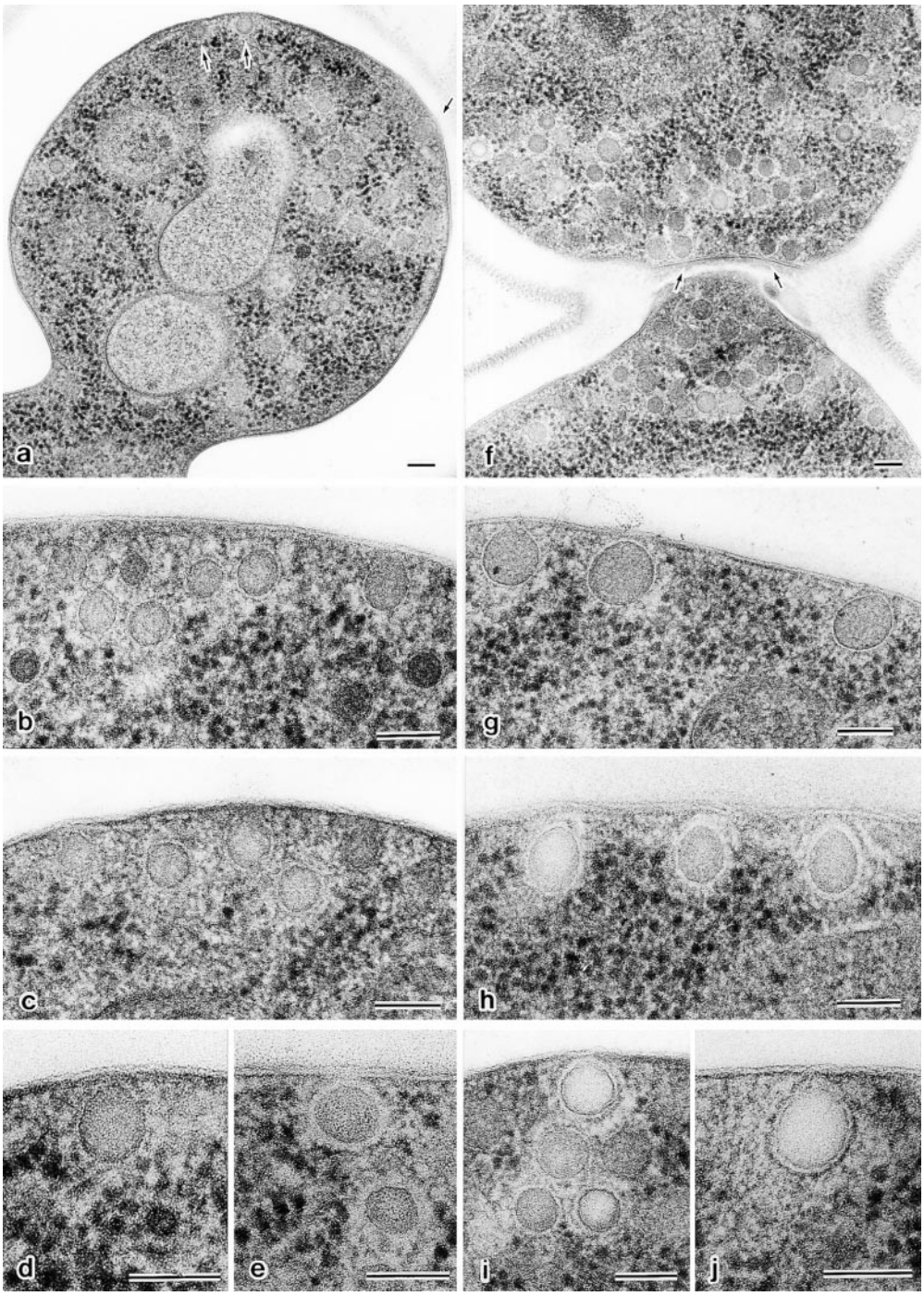


*Figure 7.* Ultrastructure of *SNC-CIIL* and *SSO-CIIL* cells. *SNC-CIIL* (a–e) and *SSO-CIIL* (f–j) cells were grown for 2 h in YP galactose and then prepared for electron microscopy by freeze-substitution. Low magnification images of a bud (a) and the septum forming between dividing mother cells (f) demonstrate an accumulation of 100-nm secretory vesicles, several of which are closely associated with the plasma membrane (see arrows). Higher magnification images (b–e, g–j) of vesicles adjacent to the plasma membrane are also shown. The vesicles in d and h evaginate towards the plasma membrane. Possible merger of the outer leaflet of the secretory vesicle with the inner leaflet of the plasma membrane can be seen in e. Bars, 100 nm.

advantage of this assay is that effects on exocytosis can be observed immediately after adding LPC, thereby minimizing the possibility of being misled by indirect effects. Secretion from both *SNC-CIIL* ($P > 0.90$) and *SSO-CIIL* ($P > 0.99$) cells was stimulated upon addition of 0.3 mM 10:0 LPC (Fig. 8 a). Interestingly, LPC stimulated more $^{35}$S-p185 secretion from *SSO-CIIL* cells than from *SNC-CIIL* cells. This difference may be related to the fact that the geranylgeranyl group of Sso-CIIL is embedded in the plasma membrane where LPC acts.

However, in addition to stimulating secretion from ggSNARE-expressing cells, LPC can also inhibit secretion. Higher concentrations of LPC (>0.6 mM) inhibited secretion from ggSNARE-expressing cells. This inhibition excludes the possibility that LPC stimulates secretion from ggSNARE-expressing cells by lysing membranes. Furthermore, the possibility that LPC stimulates exocytosis from ggSNARE-expressing cells via nonspecific detergent artifacts can be excluded because 0.5% Triton X-100 and Tween 20 have no effect on p185 release (data not shown).

If a large pool of hemifused secretory vesicles accumulates in Sso-CIIL–expressing cells, addition of LPC might result in a burst of secretion. To test for this effect, the amount of $^{35}$S-p185 release in *SSO-CIIL* cells was quantified at three time points after LPC addition (Fig. 8 b). Instead of a burst of $^{35}$S-p185 release, there was a sustained increase in the secretion rate. These data suggest that only a small fraction of the secretory vesicles accumulated in

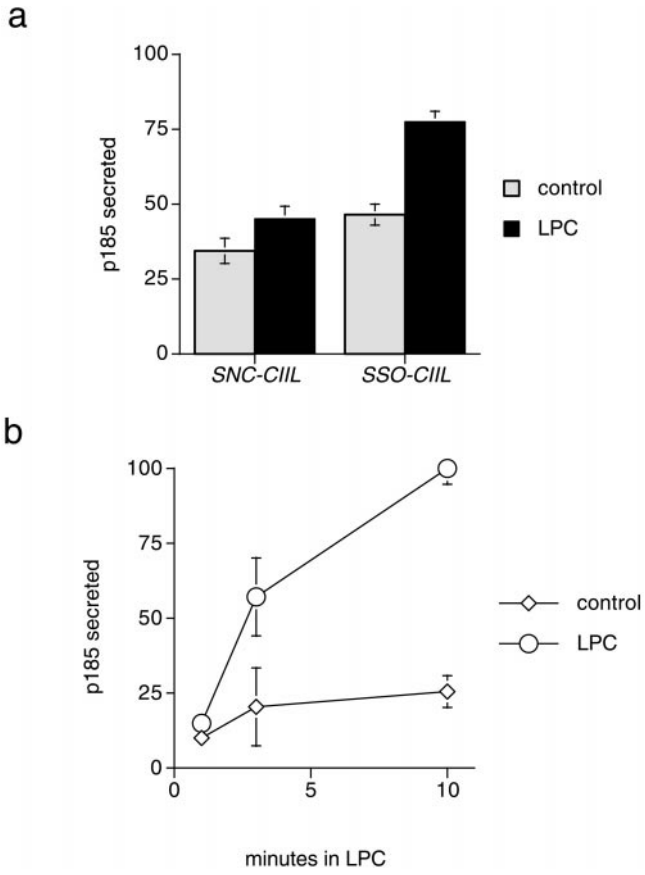


*Figure 8.* LPC-stimulated secretion. (a) *SNC-CIIL* and *SSO-CIIL* cells were pulse labeled for 5 min with [$^{35}$S]-ProMix, chased for 5 min with excess methionine, and then stimulated with 0.3 mM LPC. Secretion of $^{35}$S-p185 was quantified (error bars indicate SEM, $n = 3$). Secretion from wild-type cells not treated with LPC was defined as 100%. (b) Kinetics of secretion from LPC-stimulated cells. *SSO-CIIL* cells were pulse labeled for 5 min with [$^{35}$S]-ProMix, chased for 5 min, and then LPC was added for the indicated times. Secretion of p185 was quantified.

the *SSO-CIIL* mutant have reached the stage that is subject to activation by LPC. This may reflect a limited number of docking sites and is in agreement with the largely cytoplasmic distribution of vesicles observed by electron microscopy (Fig. 7).

## Discussion

The *SNC-CIIL* and *SSO-CIIL* mutations were designed by analogy to the GPI-HA mutant of the influenza HA fusion protein to test the hypothesis that SNARE transmembrane domains have a critical function in membrane fusion. High expression of Snc-CIIL or Sso-CIIL inhibited exocytosis, but did not inhibit transport of secretory vesicles to the bud or docking of vesicles to the plasma membrane. Instead, exocytosis was arrested at a late, LPC-sensitive stage. These observations suggest that an interaction between the transmembrane domain of SNARE proteins and the distal leaflets of apposed membranes is essential for fusion.

We propose that a functional SNARE complex must include at least two transmembrane domains, one for the vesicle membrane and one for the target membrane. Similarly, viral fusion requires both a transmembrane domain and a fusion peptide for fusion activity, and mutations in either domain can result in hemifusion (Kemble et al., 1993; Qiao et al., 1999). Several SNARE proteins are naturally modified with lipids (Hess et al., 1992; Couve et al., 1995; McNew et al., 1997; Vogel and Roche, 1999). For example, Snc1p is palmitylated on Cys95, the same site that is geranylgeranylated in Snc-CIIL (Couve et al., 1995). Nevertheless, neither overexpression of palmitylated Snc1p nor a *snc1-Cys95Ala* mutation that prevents palmitylation has a deleterious effect on secretion (Protopopov et al., 1993; Couve et al., 1995). Thus, Snc-CIIL toxicity correlates with the lack of a transmembrane domain rather that the presence of a lipid anchor. Another interesting example is Ykt6p, the Sed5p-associated v-SNARE implicated in ER to Golgi complex transport and vacuole fusion (Sogaard et al., 1994; Lupashin et al., 1997; McNew et al., 1997; Ungermann et al., 1998a). Ykt6p is attached to vesicles via a COOH-terminal farnesyl group (Sogaard et al., 1994). Since Ykt6p does not have a transmembrane domain, we suggest that Ykt6p incorporates into SNARE complexes that have a second v-SNARE protein with a transmembrane domain such as Vti1p.

Snc-CIIL and Sso-CIIL both assemble into SNARE complexes indistinguishable by several criteria from complexes containing wild-type SNAREs. These complexes can assemble into higher-order multimers, recruit GFP-Sec1p to bud tips, and be disassembled by Sec18p. Nevertheless, ggSNAREs do not interfere with the assembly of wild-type SNARE proteins into complexes. Therefore, it is the presence of the mutant SNARE complexes rather than the absence of wild-type complexes that is responsible for the inhibition of exocytosis. Assembly of Sso-CIIL into SNARE complexes indicates that vesicles have docked to the plasma membrane because the temperature-sensitive *sec5* mutation inhibited assembly of SNARE complexes containing Sso-CIIL as well as native Ssop. Sec5p is a component of the exocyst complex that is thought to tether secretory vesicles to the plasma membrane before SNARE complex assembly (Guo et al., 1999; Grote et al., 2000). Because only a short span of amino acids separates the transmembrane domains of Sncp and Ssop from their SNARE complex forming α-helical domains, the completion of SNARE complex assembly should bring the two membranes into close proximity and may also distort the membranes at the point of contact leading to the initiation of fusion (Sutton et al., 1998).

One mechanism for ggSNAREs to inhibit fusion without affecting the assembly of normal SNARE complexes is by poisoning the function of a higher-order SNARE complex. In support of this model, we found that the majority of the exocytic SNARE complexes in a yeast lysate sediment at >20S. These rapidly sedimenting complexes must contain at least two copies of Ssop because untagged Sso1p coimmunoprecipitates with HA-Sso2p from fractions near the bottom of the gradient. Furthermore, these higher-order SNARE complexes are likely to have assembled in vivo rather than in the lysate because if different populations of cells expressing myc-Ssop and HA-Sncp are mixed before lysis, the myc-Ssop and HA-Sncp do not bind to each other in vitro (Carr et al., 1999). Because Snc-CIIL toxicity requires a high ratio of Snc-CIIL to wild-type Sncp expression, higher-order SNARE complexes

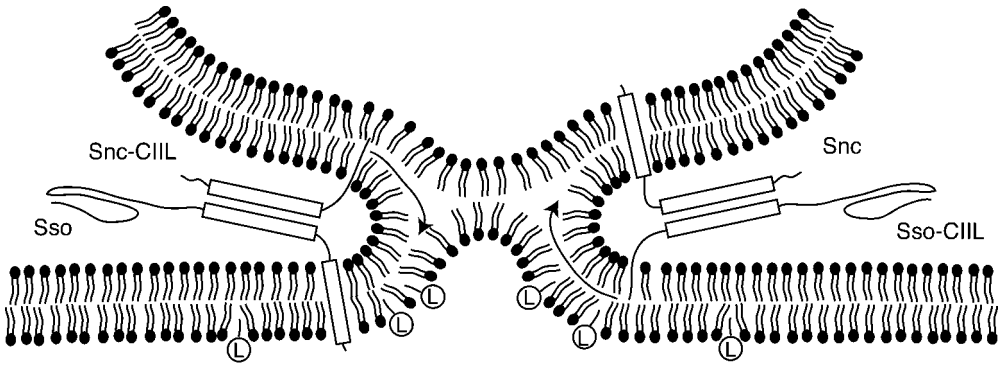


*Figure 9.* Model of LPC incorporation into the outer leaflet of the plasma membrane in ggSNARE cells arrested in hemifusion. The transmembrane domains of Snc-CIIL and Sso-CIIL (boxes) have been replaced by a geranylgeranyl lipid anchor (line). Snc-CIIL and Sso-CIIL assemble into SNARE complexes via interactions between their α-helical domains (hatched boxes). Assembly of these mutant SNARE complexes promotes hemifusion wherein the outer leaflet of the secretory vesicle fuses with the inner leaflet of the plasma membrane, but the distal leaflets remain distinct. Once hemifusion occurs, the lipidic anchors on Snc-CIIL and Sso-CIIL are free to diffuse across the lipidic stalk connecting the two membranes (arrows) and are thus unable to catalyze merger of the distal leaflets. LPC (L) added to the medium incorporates into the outer leaflet of the plasma membrane and promotes positive curvature in one leaflet of the hemifusion diaphragm. This positive curvature reduces the activation energy for fusion of the distal leaflets, thereby stimulating completion of the exocytic reaction.

may retain partial function if only a minority of the Snc proteins have lipid anchors. Similarly, viral fusion involves cooperative interactions between multiple HA trimers (Blumenthal et al., 1996; Danieli et al., 1996), but based on theoretical calculations, less than half of these HA trimers must undergo a conformational shift for fusion to occur (Bentz, 2000).

To test the hypothesis that ggSNAREs and GPI-HA are defective at a similar stage of fusion, we tested whether LPC would stimulate exocytosis. LPC, which induces positive curvature in the outer leaflet of the plasma membrane, stimulated secretion from ggSNARE-expressing cells. Similarly, chlorpromazine, which induces positive curvature in the inner leaflet of the plasma membrane, stimulates fusion of GPI-HA–expressing fibroblasts with red blood cells (Melikyan et al., 1997; Chernomordik et al., 1999). In the absence of chlorpromazine, GPI-HA mediates hemifusion, the fusion of the proximal leaflets of two membranes but not their distal leaflets. Thus, our data support the model that ggSNAREs are defective at the final stage of exocytic fusion—the merging of the inner leaflet of the secretory vesicle with the outer leaflet of the plasma membrane (Fig. 9). However, because it is not possible to selectively label the outer leaflet of secretory vesicles with a fluorescent marker in living cells, there is no definitive evidence that ggSNAREs induce hemifusion. Also, in contrast to the consistent observation that LPC stimulates secretion from ggSNARE-expressing cells, in wild-type cells LPC slightly inhibited secretion in some experiments and stimulated secretion in others. These disparate results suggest that the transition from hemifusion to complete fusion may be rate limiting in wild-type cells under appropriate conditions.

We considered several alternative explanations for the mechanism of LPC stimulation. LPC might interact with proteins rather than lipids (Gunther-Ausborn et al., 1995). Since LPC inhibits several enzymes including adenyl cyclase in yeast (Resnick and Tomaska, 1994), it is possible that LPC stimulates fusion by interacting with a protein. However, LPC does not cross the yeast plasma membrane (Tang et al., 1996), so it would not have access to cytoplasmic proteins including those involved in membrane fusion. Although LPC might exert effects on the cytoplasmic side of the plasma membrane via a cell surface receptor, there is no evidence for LPC receptors or ligand-stimulated exocytosis in yeast.

LPC stimulated release of 58% of the accumulated $^{35}$S-p185 in *SSO-CIIL* cells and 16% in *SNC-CIIL* cells. Perhaps, the effectiveness of LPC is limited by our experimental system. First, LPC has direct access to only one leaflet of the putative hemifusion diaphragm. LPC might enter the inner leaflet of secretory vesicles after recycling from the plasma membrane to the Golgi by endocytosis, but this LPC cannot stimulate $^{35}$S-p185 release in our experiments because secretory vesicles are loaded with $^{35}$S-p185 before the addition of LPC. Second, there is a massive buildup of secretory vesicles in the cells before the $^{35}$S–amino acid pulse. These vesicles are likely to be sequestering some of the components involved in vesicle targeting and fusion. For comparison, addition of 0.4 mM chlorpromazine to a GPI-HA fusion assay resulted in full fusion of only 36% of the cells (Melikyan et al., 1997). Thus, we consider the partial rescue of secretion by LPC to be highly significant.

One unresolved question is why a large number of SNARE complexes, docked secretory vesicles, and perhaps hemifusion intermediates, did not accumulate in the ggSNARE-expressing cells if secretion is blocked at a stage after vesicle docking. One possibility is that docking and hemifusion are reversible. Interestingly, a reversible hemifusion intermediate has been detected for hemifusion catalyzed by HA (Leikina and Chernomordik, 2000). However, there is some evidence that SNARE complex assembly is not reversible. If *sec5-24 SSO-CIIL* cells are grown for 11 h in YP galactose to completely inhibit secretion, there is no reduction in SNARE complex levels upon shifting to 37°C (our unpublished observation). Since Sec5p is required for assembly of exocytic SNARE complexes, and SNARE complex levels do not decrease in this situation, there must also be no SNARE complex disassembly. The implication of this result is that there is a small, stable population of docked secretory vesicles rather than a continuous cycle of vesicle docking and undocking. An alternative explanation for the failure of docked vesicles to accumulate is that there are a limited number of secretory vesicle docking sites on the plasma

membrane. Since there are large unassembled pools of all of the known secretory proteins (SNAREs, Sec1p, the exocyst, and Sec4p), availability of these proteins is not likely to be limiting for vesicle docking. Thus, we suggest that the number of docking sites is limited either by an unknown component or by a sensor of assembled SNARE complexes that negatively regulates vesicle docking.

The hypothesis that SNAREs catalyze membrane fusion has been challenged by two groups who have reported that SNARE complexes can be disassembled before membrane fusion (Coorssen et al., 1998; Tahara et al., 1998; Ungermann et al., 1998b). They have proposed that SNAREs stabilize vesicle docking and recruit other factors that catalyze fusion. We find that ggSNAREs assemble into SNARE complexes, dock secretory vesicles to plasma membrane, and recruit GFP-Sec1p to exocytic sites, yet still block fusion. To conform to the alternative hypothesis, the transmembrane domains of both Sncp and Ssop must be essential to recruit the alternative fusion protein. Thus, our data are more consistent with the model that SNARE complexes directly catalyze fusion.

We would like to thank Dr. Mary Munson (Princeton University, Princeton, New Jersey) for purified cytoplasmic domains of Sncp and Ssop, Drs. Leonid Chernomordik (National Institutes of Health, Bethesda, MD), Fred Cohen (Rush Medical College, Chicago, IL), and Yu Jiang (Princeton University) for helpful discussion, and Dr. Judith White (University of Virginia, Charlottesville, VA) for critical comments on the manuscript.

The electron microscopy for this study was performed in the Electron Microscopy Facility of the Japan Woman's University, directed by Dr. M. Osumi. This work was supported by a National Institutes of Health grant to Peter J. Novick.

Submitted: 29 March 2000
Revised: 7 September 2000
Accepted: 7 September 2000

### *References*

Abeliovich, H., E. Grote, P. Novick, and S. Ferro-Novick. 1998. Tlg2p, a yeast syntaxin homolog that resides on the Golgi and endocytic structures. *J. Biol. Chem.* 273:11719–11727.

Baba, M., M. Osumi, S.V. Scott, D.J. Klionsky, and Y. Ohsumi. 1997. Two distinct pathways for targeting proteins from the cytoplasm to the vacuole/lysosome. *J. Cell Biol.* 139:1687–1695.

Bentz, J. 1993. Viral Fusion Mechanisms. CRC Press, Boca Raton, FL. 529 pp.

Bentz, J. 2000. Minimal aggregate size and minimal fusion unit for the first fusion pore of influenza hemagglutinin-mediated membrane fusion. *Biophys. J.* 78:227–245.

Bittner, M.A., M.K. Bennett, and R.W. Holz. 1996. Evidence that syntaxin 1A is involved in storage in the secretory pathway. *J. Biol. Chem.* 271:11214–11221.

Blumenthal, R., D.P. Sarkar, S. Durell, D.E. Howard, and S.J. Morris. 1996. Dilation of the influenza hemagglutinin fusion pore revealed by the kinetics of individual cell–cell fusion events. *J. Cell Biol.* 135:63–71.

Carr, C.M., E. Grote, M. Munson, F.M. Hughson, and P.J. Novick. 1999. Sec1p binds to SNARE complexes and concentrates at sites of secretion. *J. Cell Biol.* 146:333–344.

Chen, Y.A., S.J. Scales, S.M. Patel, Y.C. Doung, and R.H. Scheller. 1999. SNARE complex formation is triggered by Ca2+ and drives membrane fusion. *Cell.* 97:165–174.

Chernomordik, L.V., E. Leikina, M.M. Kozlov, V.A. Frolov, and J. Zimmerberg. 1999. Structural intermediates in influenza haemagglutinin-mediated fusion. *Mol. Membr. Biol.* 16:33–42.

Choy, E., V.K. Chiu, J. Silletti, M. Feoktistov, T. Morimoto, D. Michaelson, I.E. Ivanov, and M.R. Philips. 1999. Endomembrane trafficking of ras: the CAAX motif targets proteins to the ER and Golgi. *Cell.* 98:69–80.

Coorssen, J.R., P.S. Blank, M. Tahara, and J. Zimmerberg. 1998. Biochemical and functional studies of cortical vesicle fusion: the SNARE complex and $Ca^{2+}$ sensitivity. *J. Cell Biol.* 143:1845–1857.

Couve, A., V. Protopopov, and J.E. Gerst. 1995. Yeast synaptobrevin homologs are modified posttranslationally by the addition of palmitate. *Proc. Natl. Acad. Sci. USA.* 92:5987–5991.

Danieli, T., S.L. Pelletier, Y.I. Henis, and J.M. White. 1996. Membrane fusion mediated by the influenza virus hemagglutinin requires the concerted action of at least three hemagglutinin trimers. *J. Cell Biol.* 133:559–569.

Dascher, C., J. Matteson, and W.E. Balch. 1994. Syntaxin 5 regulates endoplasmic reticulum to Golgi transport. *J. Biol. Chem.* 269:29363–29366.

Gaynor, E.C., and S.D. Emr. 1997. COPI-independent anterograde transport: cargo-selective ER to Golgi protein transport in yeast COPI mutants. *J. Cell Biol.* 136:789–802.

Govindan, B., R. Bowser, and P. Novick. 1995. The role of Myo2, a yeast class V myosin, in vesicular transport. *J. Cell Biol.* 128:1055–1068.

Grote, E., and P.J. Novick. 1999. Promiscuity in Rab-SNARE interactions. *Mol. Biol. Cell.* 10:4149–4161.

Grote, E., C.M. Carr, and P.J. Novick. 2000. Ordering the final events in yeast exocytosis. *J. Cell Biol.* 151:439–451.

Gunther-Ausborn, S., A. Praetor, and T. Stegmann. 1995. Inhibition of influenza-induced membrane fusion by lysophosphatidylcholine. *J. Biol. Chem.* 270:29279–29285.

Guo, W., D. Roth, C. Walch-Solimena, and P. Novick. 1999. The exocyst is an effector for Sec4p, targeting secretory vesicles to sites of exocytosis. *EMBO (Eur. Mol. Biol. Organ.) J.* 18:1071–1080.

Hanson, P.I., R. Roth, H. Morisaki, R. Jahn, and J.E. Heuser. 1997. Structure and conformational changes in NSF and its membrane receptor complexes visualized by quick-freeze/deep-etch electron microscopy. *Cell.* 90:523–535.

Hess, D.T., T.M. Slater, M.C. Wilson, and J.H. Skene. 1992. The 25 kDa synaptosomal-associated protein SNAP-25 is the major methionine-rich polypeptide in rapid axonal transport and a major substrate for palmitoylation in adult CNS. *J. Neurosci.* 12:4634–4641.

Holthuis, J.C., B.J. Nichols, S. Dhruvakumar, and H.R. Pelham. 1998. Two syntaxin homologues in the TGN/endosomal system of yeast. *EMBO (Eur. Mol. Biol. Organ.) J.* 17:113–126.

Jiang, Y., G. Rossi, and S. Ferro-Novick. 1993. Bet2p and Mad2p are components of a prenyltransferase that adds geranylgeranyl onto Ypt1p and Sec4p. *Nature.* 366:84–86.

Kemble, G.W., Y.I. Henis, and J.M. White. 1993. GPI- and transmembrane-anchored influenza hemagglutinin differ in structure and receptor binding activity. *J. Cell Biol.* 122:1253–1265.

Laage, R., J. Rohde, B. Brosig, and D. Langosch. 2000. A conserved membrane-spanning amino acid motif drives homomeric and supports heteromeric assembly of presynaptic SNARE proteins. *J. Biol. Chem.* 275:17481–17487.

Leikina, E., and L.V. Chernomordik. 2000. Reversible merger of membranes at the early stage of influenza hemagglutinin-mediated fusion. *Mol. Biol. Cell.* 11:2359–2371.

Lupashin, V.V., I.D. Pokrovskaya, J.A. McNew, and M.G. Waters. 1997. Characterization of a novel yeast SNARE protein implicated in Golgi retrograde traffic. *Mol. Biol. Cell.* 8:2659–2676.

Mayer, A., W. Wickner, and A. Haas. 1996. Sec18p (NSF)-driven release of Sec17p (alpha-SNAP) can precede docking and fusion of yeast vacuoles. *Cell.* 85:83–94.

McNew, J.A., M. Sogaard, N.M. Lampen, S. Machida, R.R. Ye, L. Lacomis, P. Tempst, J.E. Rothman, and T.H. Sollner. 1997. Ykt6p, a prenylated SNARE essential for endoplasmic reticulum-Golgi transport. *J. Biol. Chem.* 272: 17776–17783.

Melikyan, G.B., S.A. Brener, D.C. Ok, and F.S. Cohen. 1997. Inner but not outer membrane leaflets control the transition from glycosylphosphatidylinositol-anchored influenza hemagglutinin-induced hemifusion to full fusion. *J. Cell Biol.* 136:995–1005.

Moores, S.L., M.D. Schaber, S.D. Mosser, E. Rands, M.B. O'Hara, V.M. Garsky, M.S. Marshall, D.L. Pompliano, and J.B. Gibbs. 1991. Sequence dependence of protein isoprenylation. *J. Biol. Chem.* 266:14603–14610.

Nichols, B.J., C. Ungermann, H.R. Pelham, W.T. Wickner, and A. Haas. 1997. Homotypic vacuolar fusion mediated by t- and v-SNAREs. *Nature.* 387:199–202.

Otto, H., P.I. Hanson, and R. Jahn. 1997. Assembly and disassembly of a ternary complex of synaptobrevin, syntaxin, and SNAP-25 in the membrane of synaptic vesicles. *Proc. Natl. Acad. Sci. USA.* 94:6197–6201.

Protopopov, V., B. Govindan, P. Novick, and J.E. Gerst. 1993. Homologs of the synaptobrevin/VAMP family of synaptic vesicle proteins function on the late secretory pathway in *S. cerevisiae*. *Cell.* 74:855–861.

Qiao, H., R.T. Armstrong, G.B. Melikyan, F.S. Cohen, and J.M. White. 1999. A specific point mutant at position 1 of the influenza hemagglutinin fusion peptide displays a hemifusion phenotype. *Mol. Biol. Cell.* 10:2759–2769.

Resnick, R.J., and L. Tomaska. 1994. Stimulation of yeast adenylyl cyclase activity by lysophospholipids and fatty acids. Implications for the regulation of Ras/effector function by lipids. *J. Biol. Chem.* 269:32336–32341.

Rice, L.M., P. Brennwald, and A.T. Brunger. 1997. Formation of a yeast SNARE complex is accompanied by significant structural changes. *FEBS Lett.* 415:49–55.

Salminen, A., and P.J. Novick. 1987. A ras-like protein is required for a post-Golgi event in yeast secretion. *Cell.* 49:527–538.

Schneider, B.L., W. Seufert, B. Steiner, Q.H. Yang, and A.B. Futcher. 1995. Use of polymerase chain reaction epitope tagging for protein tagging in *Saccharomyces cerevisiae*. *Yeast.* 11:1265–1274.

Sheetz, M.P., and S.J. Singer. 1974. Biological membranes as bilayer couples. A molecular mechanism of drug-erythrocyte interactions. *Proc. Natl. Acad. Sci. USA.* 71:4457–4461.

Skehel, J.J., and D.C. Wiley. 1998. Coiled coils in both intracellular vesicle and viral membrane fusion. *Cell.* 95:871–874.

Sogaard, M., K. Tani, R.R. Ye, S. Geromanos, P. Tempst, T. Kirchhausen, J.E. Rothman, and T. Sollner. 1994. A rab protein is required for the assembly of SNARE complexes in the docking of transport vesicles. *Cell.* 78:937–948.

Sollner, T., M.K. Bennett, S.W. Whiteheart, R.H. Scheller, and J.E. Rothman. 1993a. A protein assembly-disassembly pathway in vitro that may correspond to sequential steps of synaptic vesicle docking, activation, and fusion. *Cell.* 75:409–418.

Sollner, T., S.W. Whiteheart, M. Brunner, H. Erdjument-Bromage, S. Geromanos, P. Tempst, and J.E. Rothman. 1993b. SNAP receptors implicated in vesicle targeting and fusion. *Nature.* 362:318–324.

Sutton, R.B., D. Fasshauer, R. Jahn, and A.T. Brunger. 1998. Crystal structure of a SNARE complex involved in synaptic exocytosis at 2.4 Å resolution. *Nature.* 395:347–353.

Tahara, M., J.R. Coorssen, K. Timmers, P.S. Blank, T. Whalley, R. Scheller, and J. Zimmerberg. 1998. Calcium can disrupt the SNARE protein complex on sea urchin egg secretory vesicles without irreversibly blocking fusion. *J. Biol. Chem.* 273:33667–33673.

Tang, X., M.S. Halleck, R.A. Schlegel, and P. Williamson. 1996. A subfamily of P-type ATPases with aminophospholipid transporting activity. *Science.* 272: 1495–1497.

TerBush, D.R., T. Maurice, D. Roth, and P. Novick. 1996. The exocyst is a multiprotein complex required for exocytosis in *Saccharomyces cerevisiae*. *EMBO (Eur. Mol. Biol. Organ.) J.* 15:6483–6494.

Ungermann, C., B.J. Nichols, H.R. Pelham, and W. Wickner. 1998a. A vacuolar v-t-SNARE complex, the predominant form in vivo and on isolated vacuoles, is disassembled and activated for docking and fusion. *J. Cell Biol.* 140: 61–69.

Ungermann, C., K. Sato, and W. Wickner. 1998b. Defining the functions of trans-SNARE pairs. *Nature.* 396:543–548.

Vida, T.A., and S.D. Emr. 1995. A new vital stain for visualizing vacuolar membrane dynamics and endocytosis in yeast. *J. Cell Biol.* 128:779–792.

Vogel, K., and P.A. Roche. 1999. SNAP-23 and SNAP-25 are palmitoylated in vivo. *Biochem. Biophys. Res. Commun.* 258:407–410.

Walch-Solimena, C., R.N. Collins, and P.J. Novick. 1997. Sec2p mediates nucleotide exchange on Sec4p and is involved in polarized delivery of post-Golgi vesicles. *J. Cell Biol.* 137:1495–1509.

Weber, T., B.V. Zemelman, J.A. McNew, B. Westermann, M. Gmachl, F. Parlati, T.H. Sollner, and J.E. Rothman. 1998. SNAREpins: minimal machinery for membrane fusion. *Cell.* 92:759–772.

White, J.M., T. Danieli, Y.I. Henis, G. Melikyan, and F.S. Cohen. 1996. Membrane fusion by the influenza hemagglutinin: the fusion pore. *Soc. Gen. Physiol. Ser.* 51:223–229.

Wu, M.N., J.T. Littleton, M.A. Bhat, A. Prokop, and H.J. Bellen. 1998. ROP, the *Drosophila* Sec1 homolog, interacts with syntaxin and regulates neurotransmitter release in a dosage-dependent manner. *EMBO (Eur. Mol. Biol. Organ.) J.* 17:127–139.